Athena

Advanced Telescope for High Energy Astrophysics

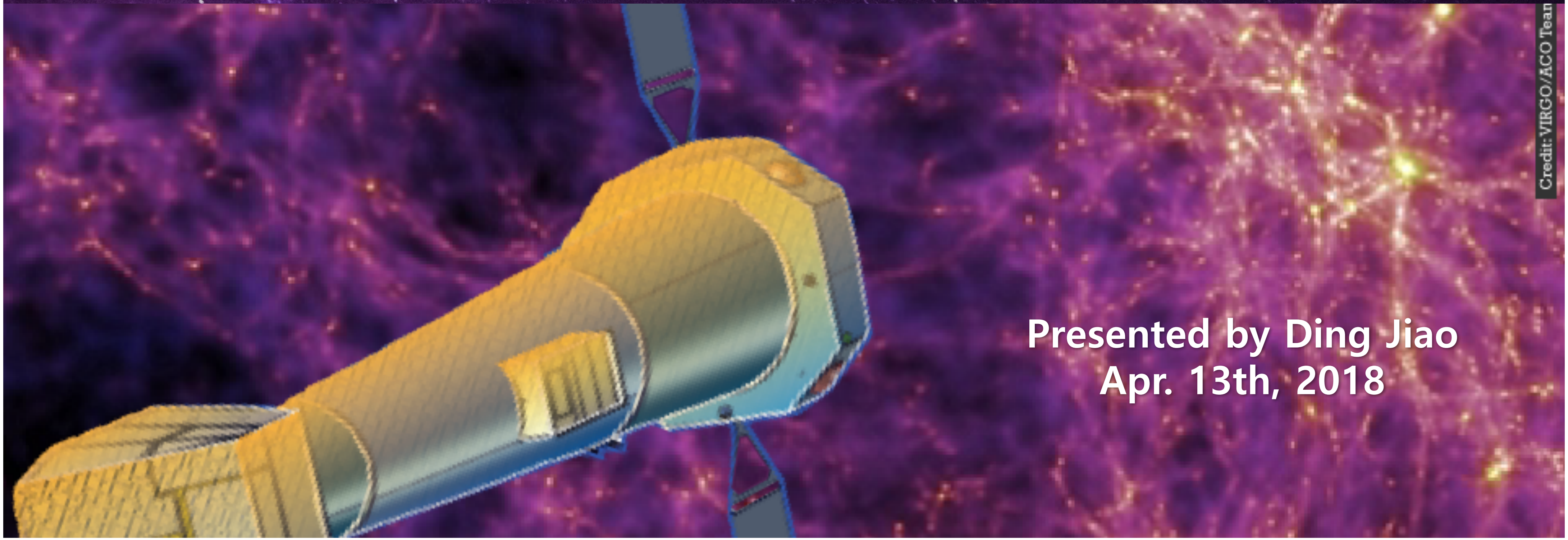

Presented by Ding Jiao
Apr. 13th, 2018

Outline

- Payload
- Science theme
- Advantages

Payload

- X-ray telescope
- X-ray Integral Field Unit (X-IFU)
- Wide Field Imager (WFI)

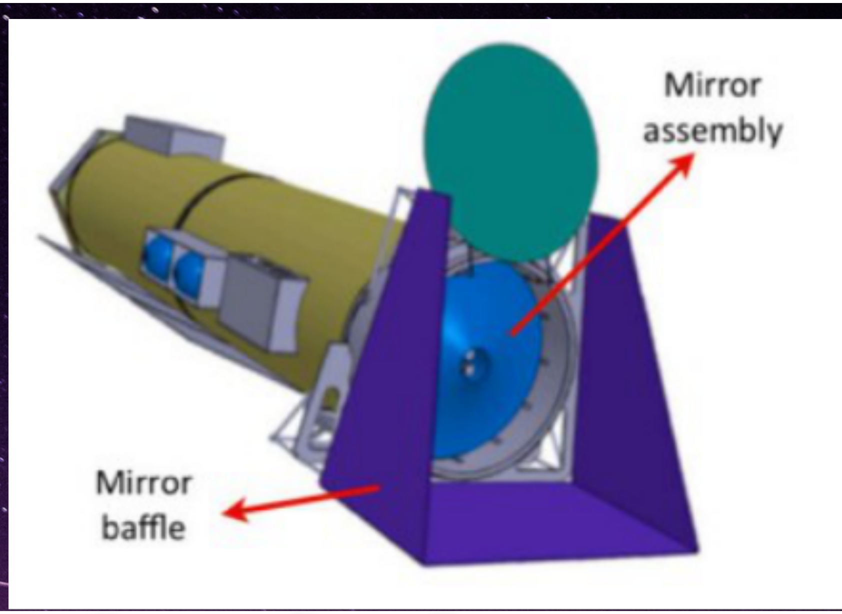

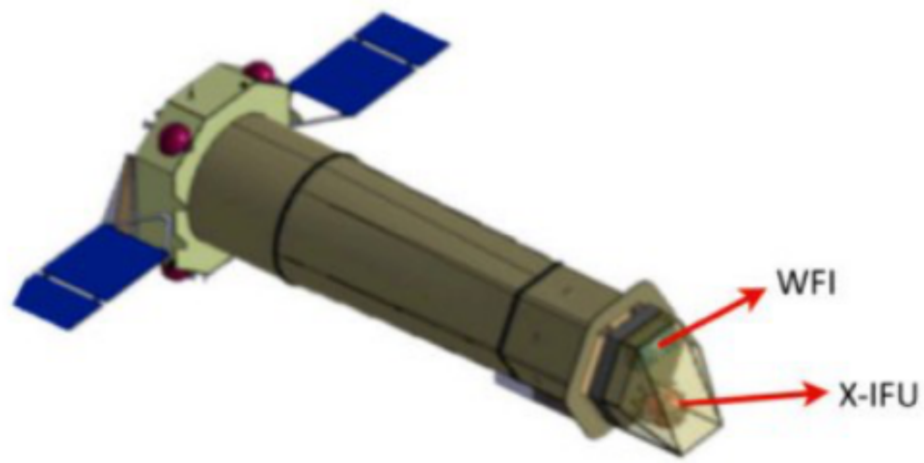

(Nandra, K., Barret, D., Barcons, X., et al. 2013)

1 Mirror

The Silicon Pore Optics technology (SPO)

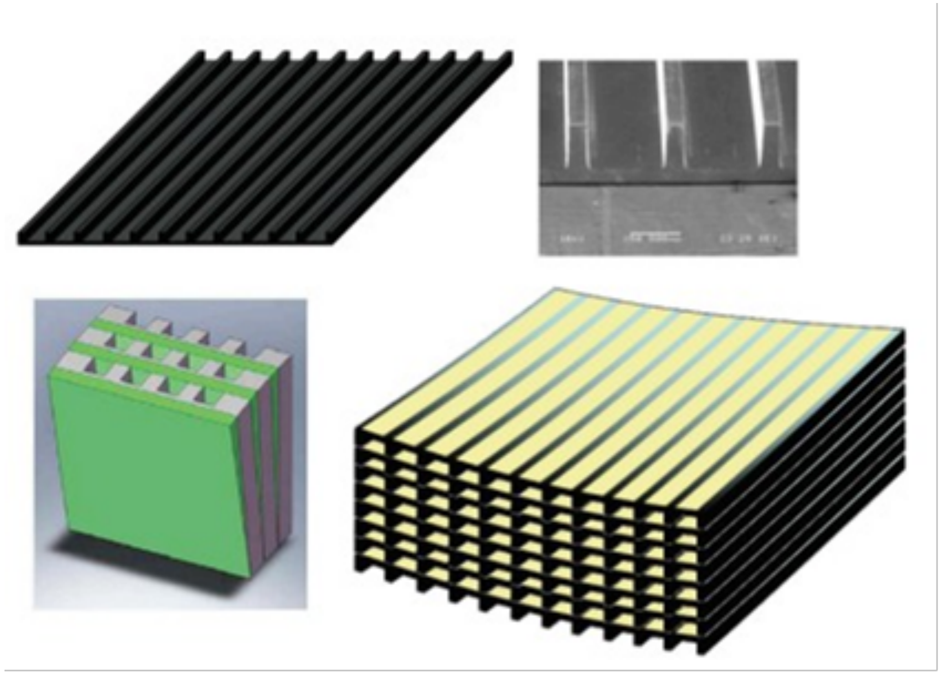

- Si wafer: 60 mm wide
- Rectangular grooves
- Thin wedge of material: in-plane focus
- High-Z material (e.g. Iridium or Gold)
- Curvature: the out-of-plane focusing

(Willingale, R., Pareschi, G., Christensen, F., den Herder, J. W. 2013)

1 Mirror

The Silicon Pore Optics technology (SPO)

Two stacks : A SPO module

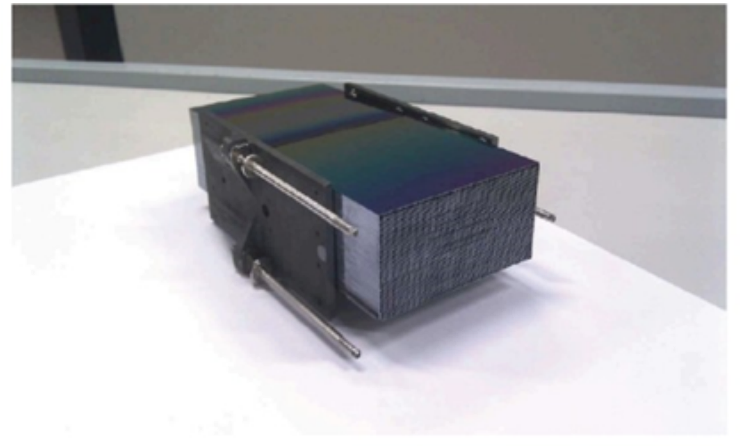

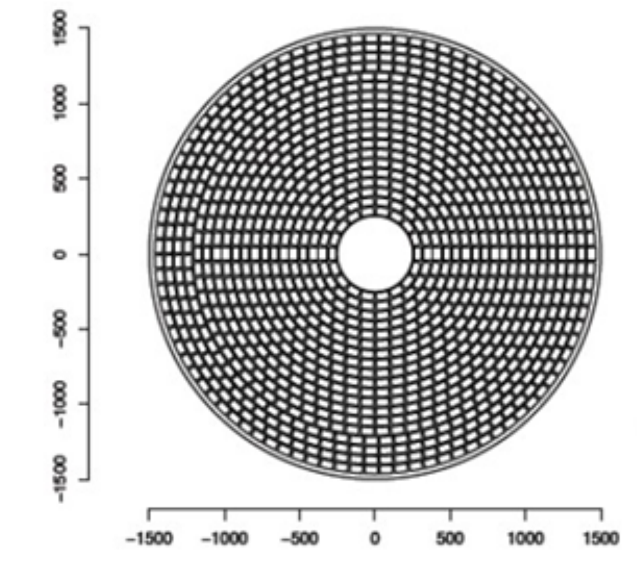

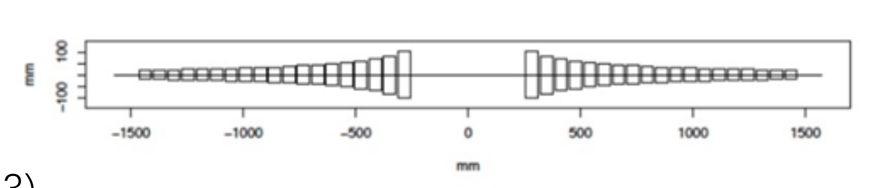

(Willingale, R., Pareschi, G., Christensen, F., den Herder, J. W. 2013)

1 Mirror

Performance

- Diameter :
  40 arc minutes
- Fixed focal length:
  12 m
- Collecting area:
  2 m^2 at 1 keV
- Angular resolution :
  5 arc seconds HEW

Very High Sensitivity
Minimal Source Confusion

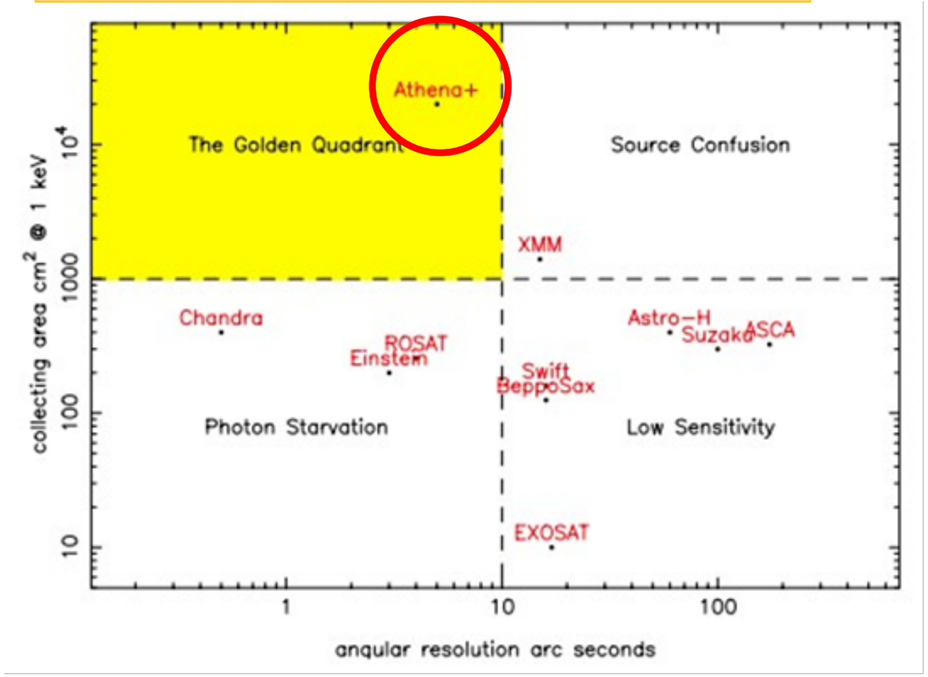

(Willingale, R., Pareschi, G., Christensen, F., den Herder, J. W. 2013)

2 X-IFU

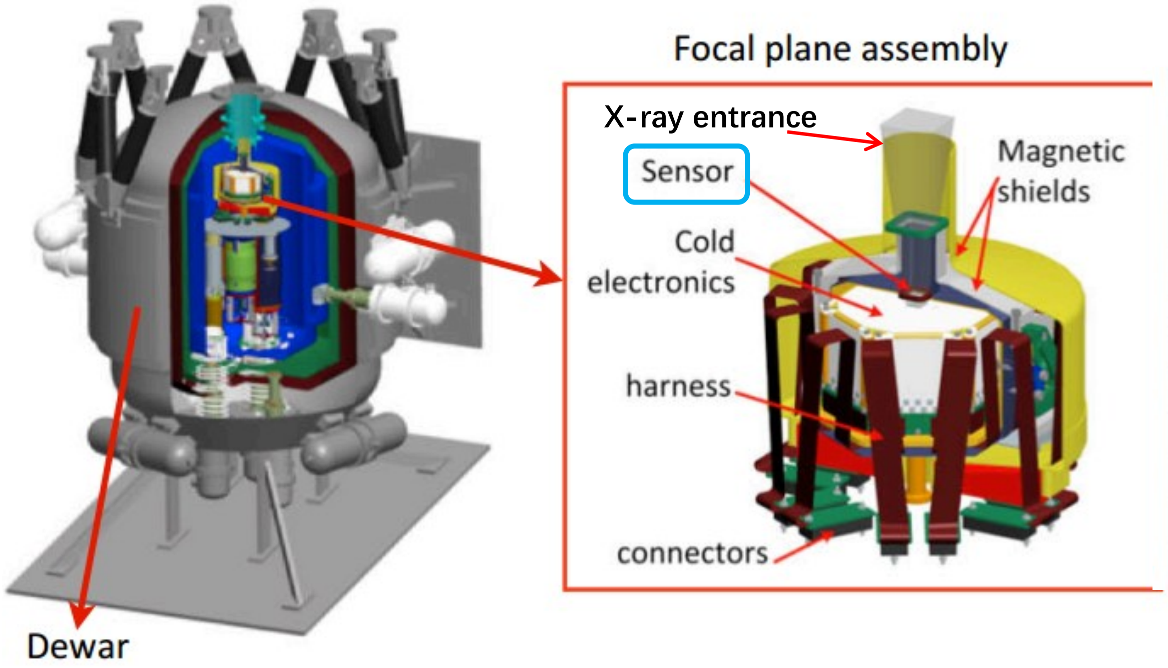

Parameter	Requirements
Energy range	0.3-12 keV
Energy resolution: E < 7 keV	2.5 eV (250 x 250 μm TES pixel)
Energy resolution: E > 7 keV	E/ΔE = 2800
Field of View	5' (diameter) (3840 TES)
Detector quantum efficiency @ 1 keV	>60%
Detector quantum efficiency @ 7 keV	>70%
Gain error (RMS)	0.4 eV
Count rate capability – faint source	1 mCrab (>80% high-resolution events)
Count rate capability – bright source	1 Crab (>30% low-resolution events)
Time resolution	10 μs
Non X-ray background	< 5 10^{-3} counts/s/cm²/keV

Effective area：1.5m^2 @1 keV

(Barret, D., den Herder, J. W., Piro, L., et al. 2013)

2 X-IFU

TES (Transition Edge Sensor)

Mo/Au bilayer

X-ray photons

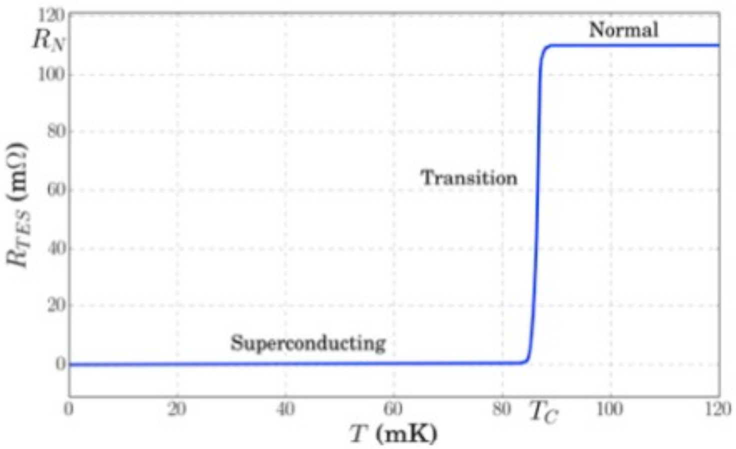

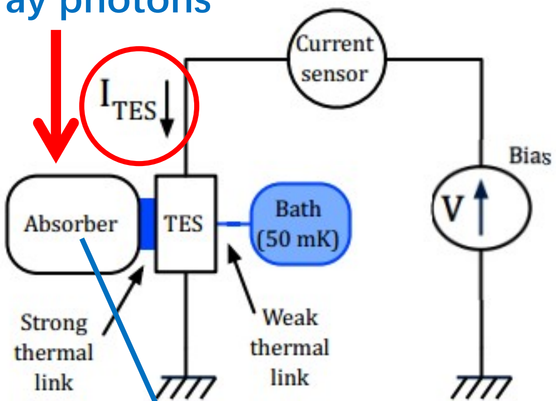

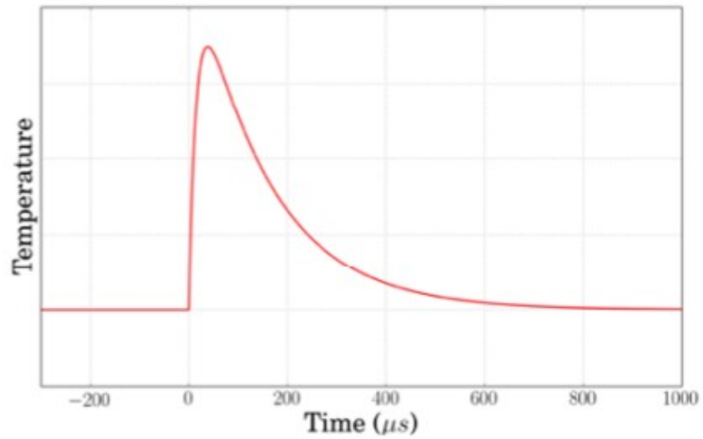

stopping power : 6 keV
low heat capacitance

(Barret, D., den Herder, J. W., Piro, L., et al. 2013)

2 X-IFU

Readout

SQUID (superconducting quantum interference device)

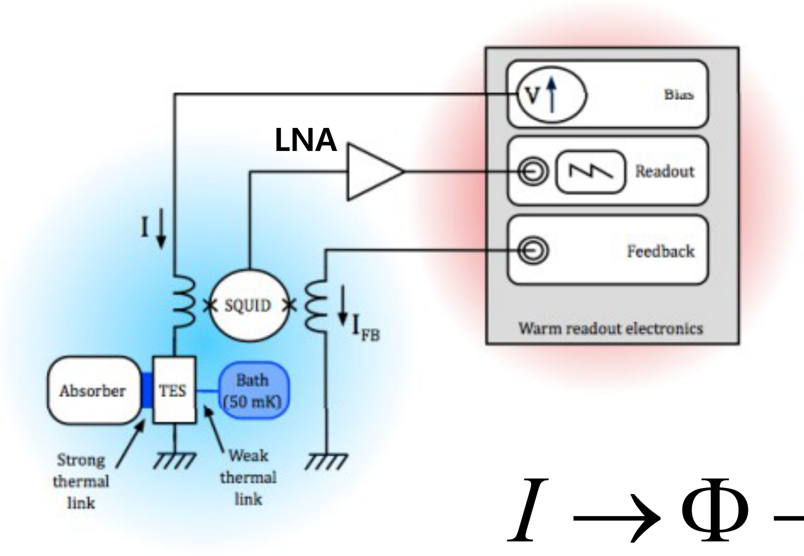

$$I \rightarrow \Phi \rightarrow V_{out}$$

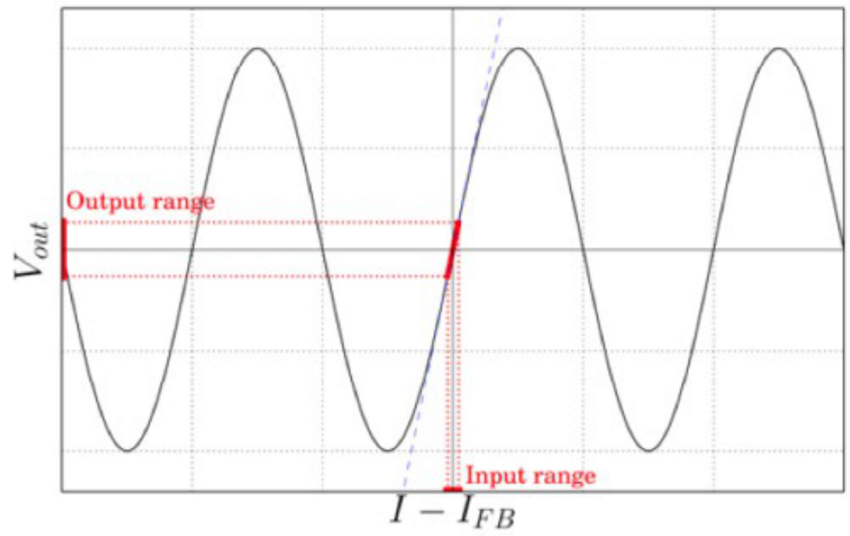

(Barret, D., den Herder, J. W., Piro, L., et al. 2013)

Frequency Domain Multiplexing (FDM)

Readout

3840 TES sensors
96 channels

range: ~1 to 5 MHz
bandwidth separation: 100 kHz

(Barret, D., den Herder, J. W., Piro, L., et al. 2013)

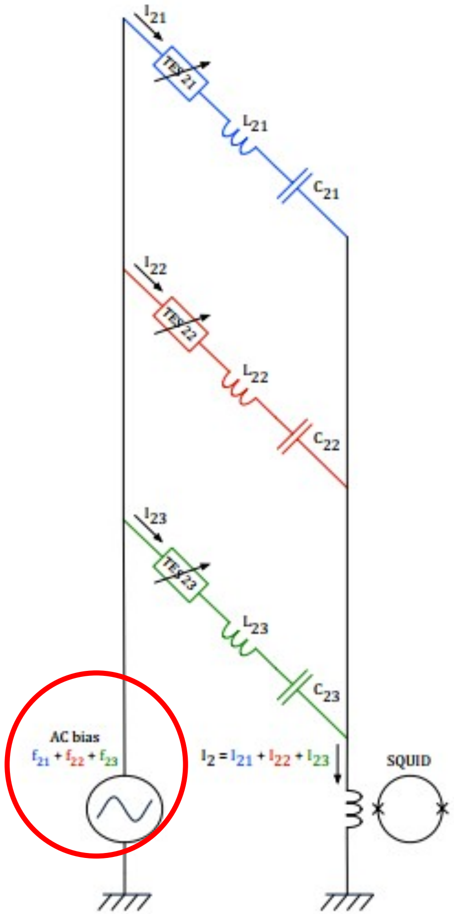

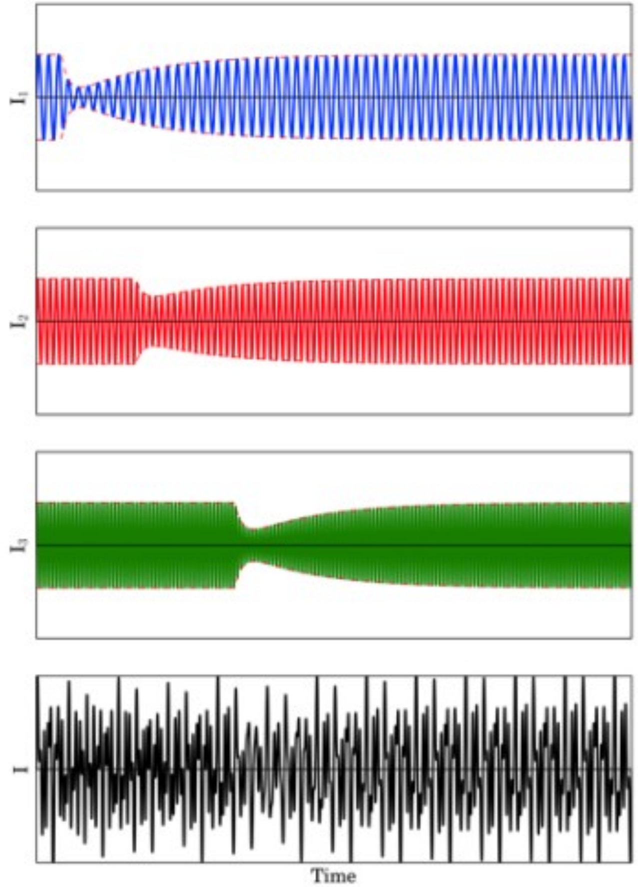

2 X-IFU

Anticoincidence

- screen the particle background
- 4 TES-array + cryogenic SQUID
  + warm electronics

- rejection rate: > 98%
  energy threshold: 20 keV
  rise time: < 30 μs.

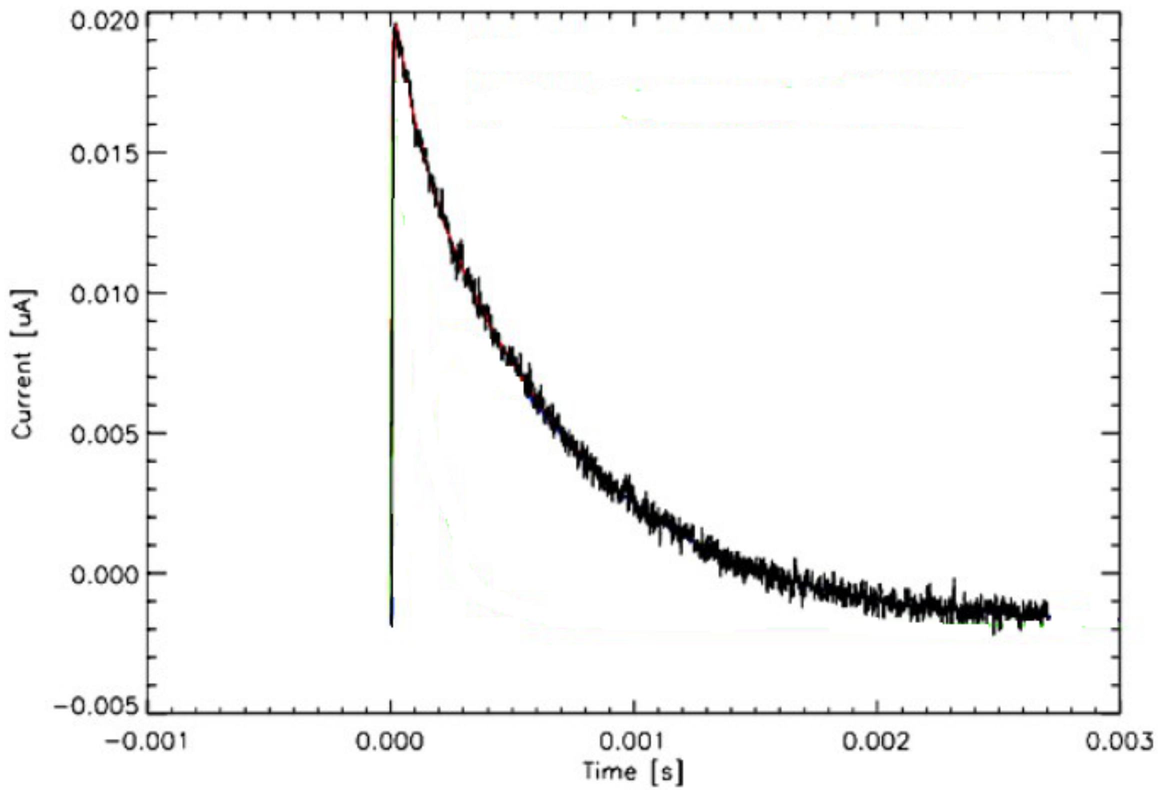

(Barret, D., den Herder, J. W., Piro, L., et al. 2013)

3 WFI

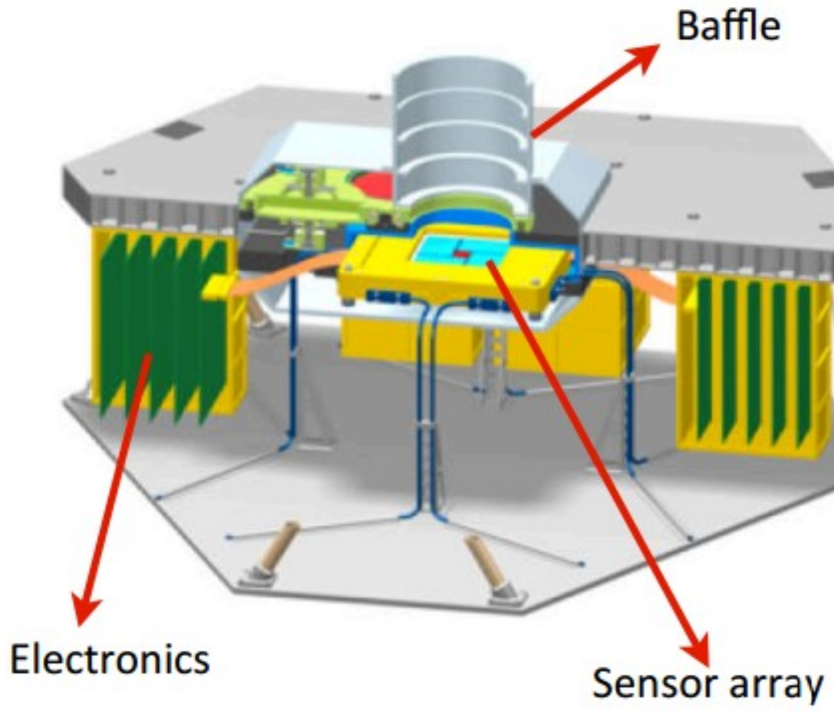

(Rau, A., Meidinger, N., Nandra, K., et al. 2013)

Parameter	Characteristic
Energy Range	0.1-15 keV
Field of View	ca. 40' x 40' (baseline) ca. 50' x 50' (goal)
Array Format	Central chip: 256 x 256 pixel Outer chips: 4x 448 x 640 pixel (baseline) 4x 576 x 768 pixel (goal)
Pixel Size	Central chip: 100 x 100 μm^2 (1.8") Outer chips: 130 x 130 μm^2 (2.3")
Angular Resolution (onaxis)	<5 arcsec (oversampling by 2.8)
Quantum efficiency (incl. optical blocking filter)	277 eV: 24% 1 keV: 87% 10 keV: 96%
Energy Resolution	ΔE < 150 eV (FWHM) @ 6 keV
Readout rate	Central chip: 7800 fps Outer chips: 2200 fps
Fast timing, count rate capability	8 μs in window mode 0.5 Crab > 88 % throughput, <3 % pile-up 1 Crab > 80 % throughput, <5 % pile-up
Particle Background at L2	3 x 10^{-4} cnt/cm²/keV/s

Effective area: ~1.7 m^2 at 1 keV

3 WFI

DEPFET (DEpleted P-channel Field Effect Transistor)

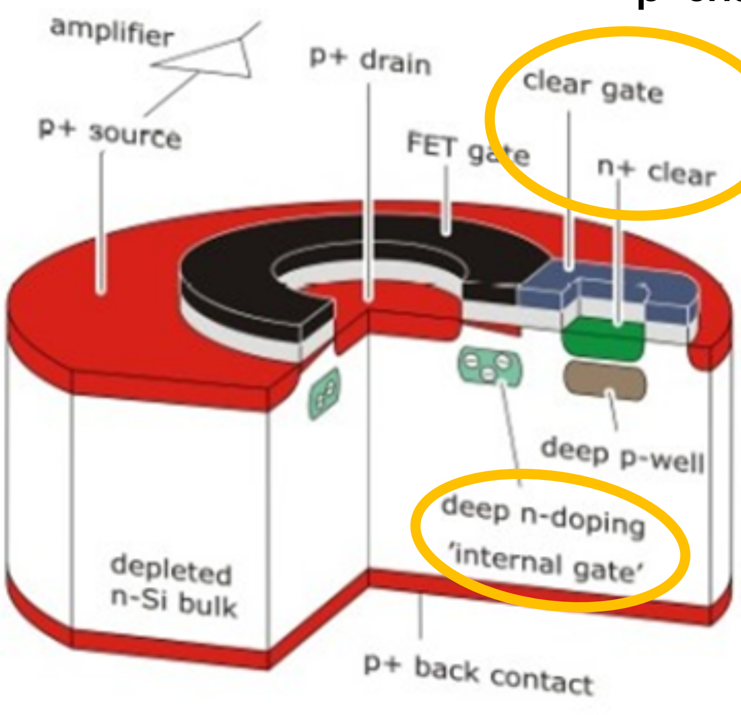

(Rau, A., Meidinger, N., Nandra, K., et al. 2013)

p-channel MetalOxide Semiconductor Field Effect Transistor (MOSFET)

integrated

depleted silicon bulk

X-ray photons

electron hole pairs

collected

internal gates

3 WFI

DEPFET (DEpleted P-channel Field Effect Transistor)

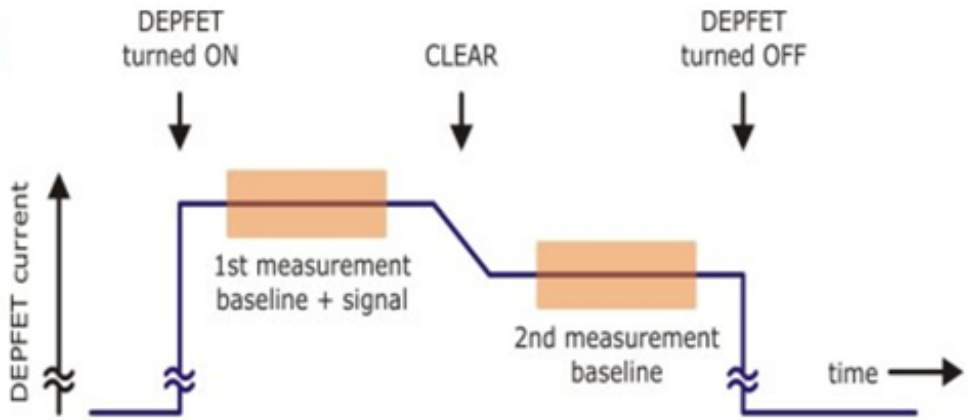

difference in conductivity

∝

the amount of charge

(Rau, A., Meidinger, N., Nandra, K., et al. 2013)

Shutter: highly n-doped contact

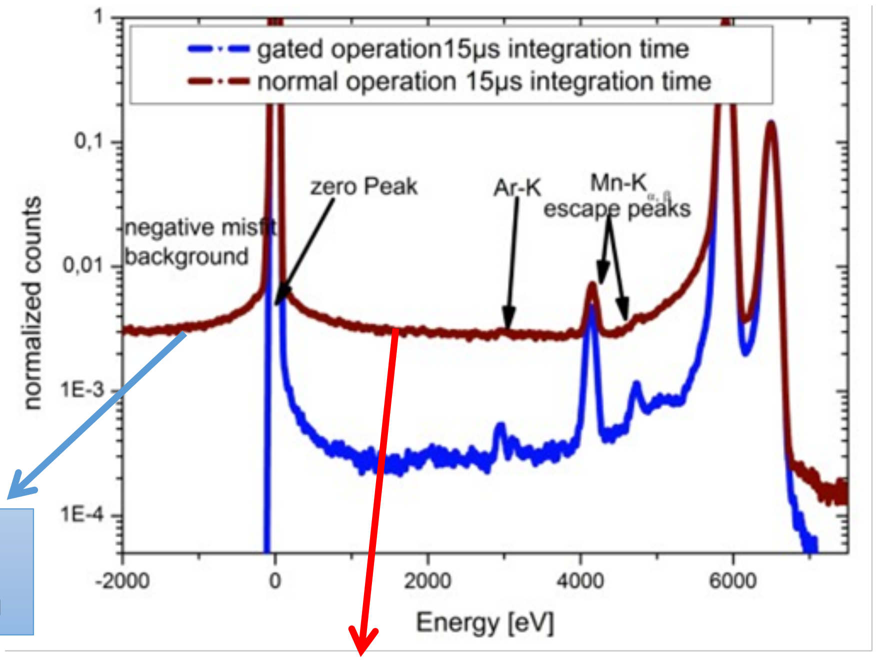

the second integration

charges deposited during the first integration

3 WFI

Focal Plane Design

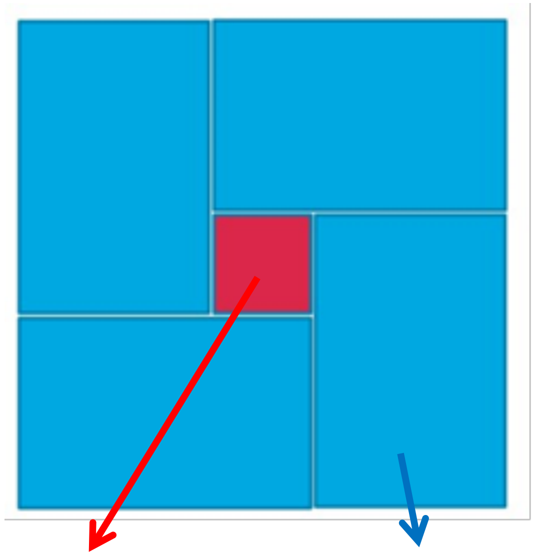

450'' x 450''

1022''x 1460''

(Rau, A., Meidinger, N., Nandra, K., et al. 2013)

Filters

- optical/UV photons

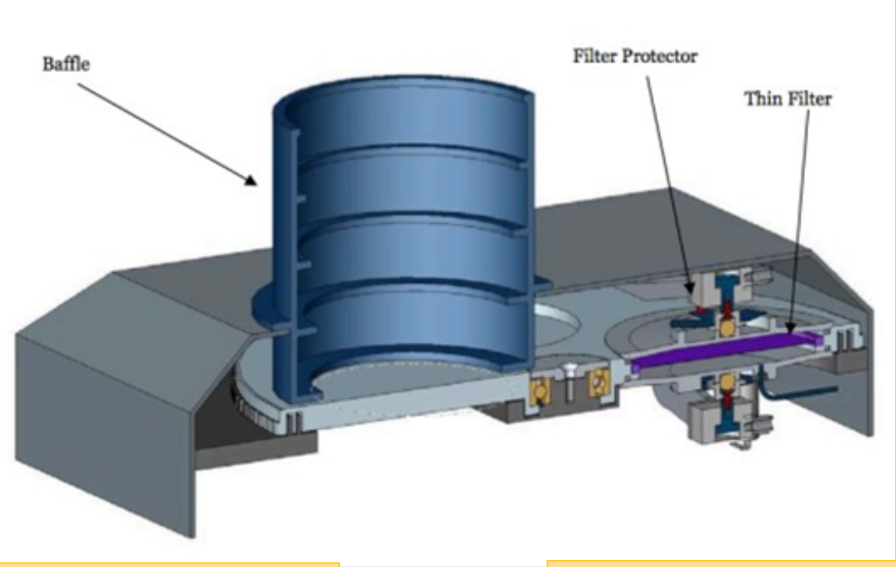

thin 70 nm Al layer

multi-layer entrance window

thin 40 nm Al-layer

350 nm polymer carrier

Science Theme

The Hot And Energetic Universe

- The Hot Universe: how does ordinary matter assemble into the large scale structures that we see today?
- The Energetic Universe: how do black holes grow and influence the Universe ?

1 The Hot Universe

The chemical history of hot baryons

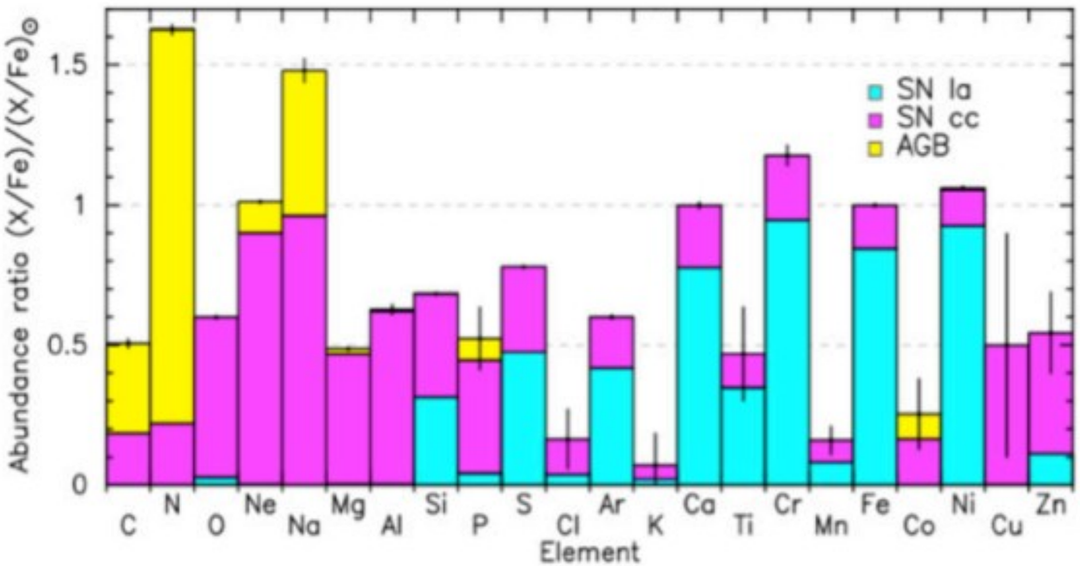

Abundance measurements for a typical cluster of galaxies (AS 1101, 100 ks)

- X-IFU X-ray spectroscopy of groups and clusters at different redshifts
- Determine where metals are produced in clusters

(Nandra, K., Barret, D., Barcons, X., et al. 2013)

2 The Energetic Universe

Formation and Early Growth of Supermassive Black Holes

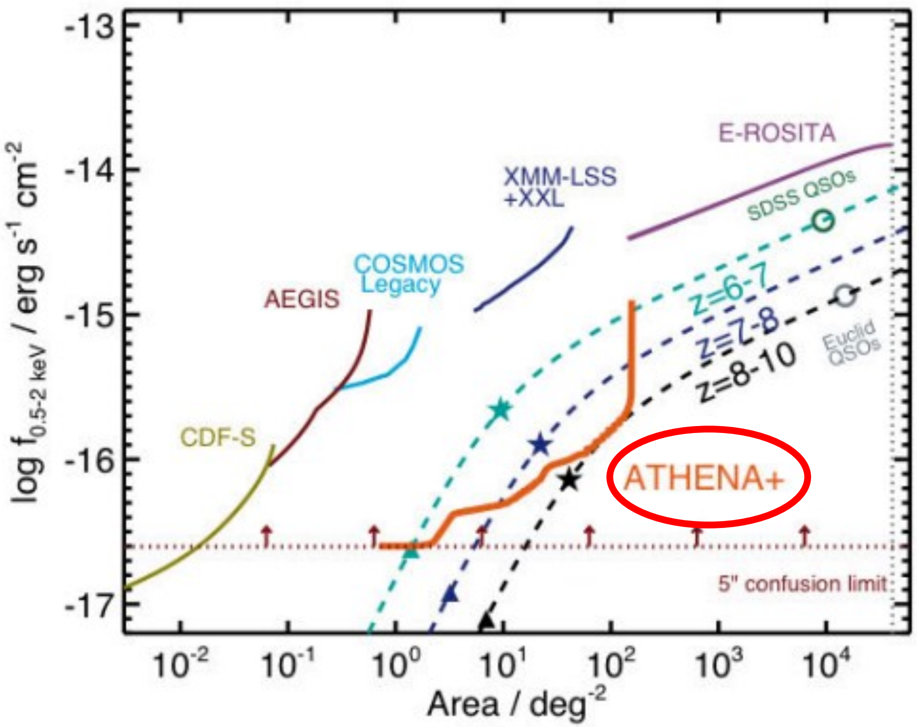

(Nandra, K., Barret, D., Barcons, X., et al. 2013)

- Discovery space
- Break through to the high redshift Universe for the first time
- Survey power: a factor ~100 better

Advantages

High-energy observational capabilities

- Superior wide field X-ray imaging capability
- High-resolution spectroscopic imaging capability
- High time resolution and count-rate capability

Advantages

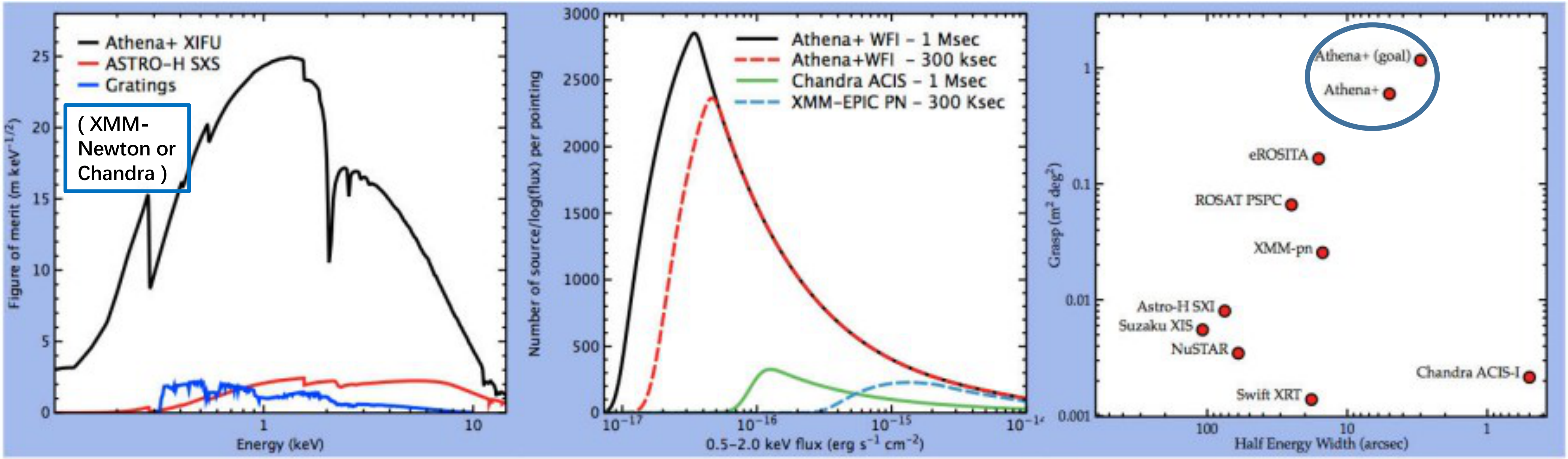

Weak spectral line detection

Number of sources

Grasp

The product of effective area at 1 keV (10 keV for NuSTAR) and the instrument field of view

(Nandra, K., Barret, D., Barcons, X., et al. 2013)

Reference

[1] Nandra, K., Barret, D., Barcons, X., et al. 2013, arXiv:1306.2307
[2] Barret, D., den Herder, J. W., Piro, L., et al. 2013, arXiv:1308.6784
[3] Rau, A., Meidinger, N., Nandra, K., et al. 2013, arXiv:1308.6785
[4] Willingale, R., Pareschi, G., Christensen, F., den Herder, J. W. 2013, arXiv:1307.1709


Thank You